Available online at www.sciencedirect.com
ScienceDirect
Applied Catalysis B: Environmental 80 (2008) 129–140
APPLIED CATALYSIS B: ENVIRONMENTAL
www.elsevier.com/locate/apcatb

Role of Re in Pt–Re/TiO_2 catalyst for water gas shift reaction: A mechanistic and kinetic study

K.G. Azzam, I.V. Babich, K. Seshan *, L. Lefferts

Catalytic Processes and Materials, Faculty of Science and Technology, IMPACT, University of Twente, P.O. Box 217, 7500AE Enschede, The Netherlands

Received 19 September 2007; received in revised form 16 November 2007; accepted 20 November 2007
Available online 22 November 2007

Abstract

Transient kinetic studies and *in situ* FTIR spectroscopy were used to follow the reaction sequences that occur during water gas shift (WGS) reaction over Pt–Re/TiO_2 catalyst. Results pointed to contributions of an associative formate route with redox regeneration and two classical redox routes involving TiO_2 and ReO_x, respectively. Under WGS reaction condition rhenium is present at least partly as ReO_x providing an additional redox route for WGS reaction in which ReO_x is reduced by CO generating CO_2 and re-oxidized by H_2O forming H_2. The overall reaction rate, based on steady state kinetics, was given by $r_{H_2} = 0.075e^{31\,kJ\,mol^{-1}/RT} \times p_{H_2O} \times p_{H_2}^{-0.5}(1-\beta)$, where β is the approach to equilibrium. Results obtained in the study indicated that the reaction between CO adsorbed on Pt and OH groups on titania is the rate-determining step.

Keywords: Water gas shift (WGS); Platinum; Rhenium; Titania; Kinetics; Reaction mechanism; Reaction orders

1. Introduction

Recently, there is a growing interest in onboard H_2 production for automobiles-fuel cells. Water gas shift (WGS) reaction, $CO + H_2O \leftrightarrow CO_2 + H_2$, $\Delta H = -41.1$ kJ/mol, is the critical step in maximizing H_2 yield from syngas, produced by steam reforming or partial oxidation of hydrocarbons [1].

Current commercial WGS technology involves multiple stages/catalysts, i.e., (i) HTS (Fe_2O_3/Cr_2O_3) and (ii) LTS ($Cu/ZnO/Al_2O_3$). This is not suitable for mobile fuel cell applications because of its technical complexity, e.g., sensitivity to startup–shutdown cycles [1–4]. There is thus tremendous interest in the development of a single stage WGS conversion. Precious metals, such as Au [5,6], Pd [7,8] or Pt [4,9–12] on different oxide supports, e.g., CeO_2 [4,6,9,11,12], ZrO_2 [4,10], TiO_2 [4,8], $Ce_xZr_{1-x}O_2$ [4,13], $Ti_xCe_{1-x}O_2$ [4] have been explored and reported to be effective for WGS. It is commonly agreed [4,12–16] that these catalysts are bi-functional wherein noble metal sorbs/activates CO and the oxide supports activate H_2O. Based on DRIFT measurements and SSITKA data, supporting evidence was obtained for the spillover mechanism of OH/H towards the noble metal and for the role of noble metal in chemisorption and activation of CO. We have shown earlier [4] that the oxide support strongly influences the catalyst performance in terms of activity and stability. For catalysts with the similar Pt loading/dispersion activity changes more than five times for different supports used. Among the catalysts tested in our study [4], Pt/TiO_2 showed the best intrinsic activity (TOF, s^{-1}), however, it deactivated with time on stream. Pt sintering was the cause of deactivation [4]. Deactivation could be overcome by adding Re to the catalyst [4]. The developed Pt–Re/TiO_2 catalyst showed excellent activity, selectivity to H_2 and stability for WGS [4].

WGS reaction is reported to occur mainly through two reaction routes, i.e., a redox [15,17,18] and an associative formate mechanism [16,19–22]. The redox mechanism involves successive reduction (by CO) and oxidation (by H_2O) of the support, while the associative mechanism involves reaction through an adsorbed surface intermediate (formate species). We have reported [23], based on transient kinetics and *in situ* FTIR studies, that WGS reaction mechanism is complex and depends strongly on the nature of the oxide supports and experimental conditions. An associative formate route with a redox regeneration of the oxide support was suggested as an

* Corresponding author. Fax: +31 53 489 4683.
E-mail address: k.seshan@utwente.nl (K. Seshan).

0926-3373/$ – see front matter © 2007 Elsevier B.V. All rights reserved.
doi:10.1016/j.apcatb.2007.11.015

additional possibility. The difference between this and the conventional ''associative formate route'' is that the conversion of surface formate to H_2 and CO_2 occurs using oxygen from titania in the former while it is from water in the latter. In the case of Pt/TiO_2 (Fig. 1), we found that WGS reaction follows both (i) a redox and (ii) an associative formate with redox regeneration routes [23].

It is generally accepted that addition of Re to Pt/TiO_2 causes significant improvement in the catalytic activity [4,8,10,24,25]. However, there is still debate about the reason for the higher activity of $Pt–Re/TiO_2$ compared to Pt/TiO_2 despite the efforts by Iida and Igrashi [10,24] and Sato et al. [8,25]. The objective of this study is to establish the reaction sequences that occur in presence of Re and to understand the role of Re in $Pt–Re/TiO_2$ for WGS reaction.

2. Experimental

2.1. Catalyst preparation

Titania (P25, Degussa) supported Pt and Re catalysts (0.5 wt% Pt/TiO_2, 0.5 wt% Re/TiO_2, 0.5 wt% Pt–0.5 wt% Re/TiO_2 and 0.3 wt% Pt–0.3 wt% Re/TiO_2) were prepared by wet impregnation, details of which are described elsewhere [4]. 5 wt% Pt/carbon (Activated Carbon, Norrit, ROX 0.8, 1100 $m^2\ g^{-1}$) catalyst was prepared by wet impregnation of the carbon with aqueous solution of H_2PtCl_6 (Aldrich). The bimetallic (5 wt% of each) Pt–Re/C was prepared by sequential impregnation without intermediate drying or calcination. Carbon was first contacted with the required concentration of NH_4ReO_4 (Aldrich) in water for 1 h with continuous stirring. Solution of H_2PtCl_6 was then added and allowed to equilibrate for 1 h. Both catalysts (Pt/C and Pt–Re/C) were then dried at 75 °C for 2 h under vacuum in a rotary evaporator. Subsequently, the catalysts were reduced in H_2 at 300 °C (10% H_2/Ar, heating rate 10 °C min^{-1}) for 4 h. For all of the experiments described below, the gases (He, H_2, CO, and CO_2) used were of >99.9% purity.

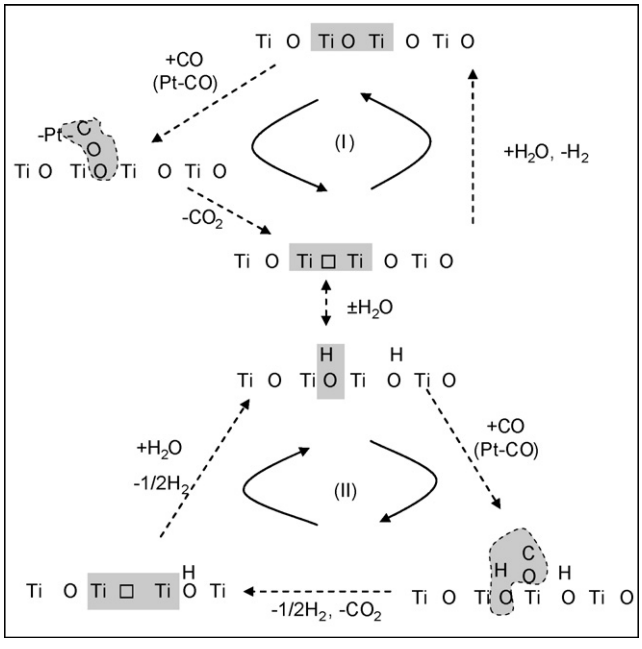

Fig. 1. WGS reaction pathways over Pt/TiO_2 catalyst as proposed in [22]: (I) redox cycle and (II) formate with redox regeneration.

2.2. Characterization

Surface areas were measured with N_2 physisorption using a Micromeritics ASAP 2400 device and applying the BET method. Pt loading was determined using a Philips PW 1480 X-ray fluorescence spectrometer.

FTIR spectra were recorded on self-supported catalyst pellets (about 10 mg of the catalyst) under flow conditions (5% CO/He, 10% H_2O/He and (5% CO + 10% H_2O)/He) at 300 °C using a Bruker Vector 22 with MCT detector. Pulse experiments were mimicked by fast switching between He and a mixture of He containing CO or H_2O. The catalyst pre-treatment was similar to catalytic test experiments. Spectra are presented in absorbance units. The empty IR cell was used as a background spectrum.

Pt dispersion was measured with CO chemisorption at room temperature using a Micromeritics Chemisorb 2750. The amount of sample used for each measurement was ~250 mg. Prior to measuring the CO uptake, the samples were reduced in pure H_2 (99.9%) from room temperature to 300 °C at a rate of 10 °C/min, flushed with He at 425 °C for 1 h and then cooled to room temperature (25 °C) in He. The CO uptake measurements were conducted at room temperature by injecting a series of pulses containing 1 mL of CO into a He stream flowing over the sample at a rate of 25 mL/min and measuring the amount of CO adsorbed per pulse. Our IR results on $Pt–Re/TiO_2$ showed, in agreement with finding of Peick et al. [26], that at room temperature, CO was only adsorbed on Pt.

2.3. Pulse experiments

Pulse transient experiments were performed at 300 °C at atmospheric pressure using a fixed-bed reactor, details of which are described elsewhere [4,22]. The catalyst (about 50 mg) was first reduced at 300 °C in 10 vol% H_2/He, 30 mL/min flow for 1 h. After this it was heated at 330 °C in He (30 mL/min) for 30 min. After cooling down to 300 °C the catalyst was contacted with fixed amounts of reactant gases using He as a carrier gas. Amount of CO in each pulse was 3.9 μmol. H_2O (1.0 μL) was injected manually directly into the reactor using a microsyringe. Pulses were repeated until the responses for reactants and products no longer changed. To determine the products formed, the outlet of the reactor was directly connected to a Porapak column (5 m, 100 °C) and a thermal conductivity detector (TCD). Downstream to the TCD detector, gases were analyzed by an online mass spectrometer (Balzers QMS 200 F). Quantitative determination of all gaseous products, except of H_2 and H_2O, was obtained from TCD data with accuracy not below ±0.1 μmoles g_{cat}^{-1}. H_2 was detected by MS; the data for H_2 are semiquantitative and comparison in H_2 formation between catalysts is not applicable.

Table 1
Properties of the catalysts

Catalyst	BET (m^2/g)	Pt/Re contents[a] (wt%)	Pt dispersion[b] (%)	TOF (s^{-1}) of H_2 formation at 300 °C	TOF (s^{-1}) of H_2 formation at 280 °C	Stability[c]
Pt/TiO_2	48	0.49	49	10	8	–
$Pt–Re/TiO_2$	49	0.50/0.48	50	15	12	+
$Pt–Re/TiO_2$	n.m.	0.34/0.26	58	16	13	n.m.
Re/TiO_2	48	0.52	–	No activity	No activity	n.a.
Pt/C[d]	n.m.	5.2	15	No activity	No activity	n.a.
Pt–Re/C[d]	n.m.	4.9/5.4	18	n.m.	n.m.	n.m.

[a] Measured by XRF.
[b] Measured by CO chemisorption at 25 °C.
[c] Pt/TiO_2 lost 40% of initial activity in 20 h testing [4], n.a.: not applicable, n.m.: not measured.
[d] Carbon surface area of 1100 m^2g^{-1}.

2.4. Catalytic test

Catalytic tests for WGS reaction were carried out in a fixed bed quartz tubular reactor (3 mm i.d.) under differential conditions, details of the setup used are described elsewhere [4]. All catalysts were first reduced in 10% H_2 in N_2 (total flow was 100 mL/min) for 30 min and subsequently purged with N_2 for another 30 min at 300 °C. A gas mixture containing 3 vol% CO, 7.5% H_2O and N_2 balance was used for catalytic tests. The feed was adjusted in bypass mode to obtain constant $CO/H_2O/N_2$ (=3/7.5/89.5 mol/mol%, N_2 as an internal standard) before the experiment. For kinetic measurements partial pressures of one of the reactants or products was varied while keeping concentrations of the other components constants (see Appendix A—Table A.1). The partial pressures were selected taking into account application of the catalyst in a WGS-membrane reactor, removing H_2 and consequently increasing CO_2 concentration axially. The total flow rate of the feed gas into the reactor was kept at 350 mL/min using Brooks mass flow controllers. The inlet and outlet gases (CO, CO_2, H_2, H_2O, and N_2) were analyzed using Varian Micro GC (CP4900) using MS5 and PPQ columns. The conversion of CO was kept below 15% to be close to differential conditions.

3. Results

3.1. Catalysts characterization and WGS reaction performance

Table 1 gives details of the characteristics of the catalysts and their catalytic performance. BET surface areas were similar for all TiO_2-based catalysts (48 ± 1 m^2/g) indicating no effect of Pt or Re impregnation on the surface area of TiO_2. The metal contents of the catalysts were close to the values expected from preparation procedures, i.e., 0.5 ± 0.04 wt% for Pt/TiO_2, Re/TiO_2, and $Pt–Re/TiO_2$ catalysts. Both Pt/TiO_2 and $Pt–Re/TiO_2$ showed similar Pt dispersions (50 ± 3%), no influence of the presence of Re on Pt dispersion was observed. For Pt/C and Pt–Re/C catalysts, the metal loadings (Pt, Re) were higher 5 ± 0.4 wt% (Table 1). We used higher loading of Pt and Re to increase catalyst activity and have an observable WGS rate in the case of Pt–Re/C, if any. Pt/C and Pt–Re/C catalyst showed Pt dispersion of about 15 ± 3%.

It can be seen from Table 1 that Re/TiO_2 catalyst showed no activity in WGS reaction. However, $Pt–Re/TiO_2$ showed higher catalytic activity than Pt/TiO_2; intrinsic activity for H_2 formation ($TOF_{300°C}$. s^{-1}) increased from 10 s^{-1} for Pt/TiO_2 to 15 s^{-1} for $Pt–Re/TiO_2$. The addition of Re to Pt/TiO_2 also improved the stability of the catalyst. $Pt–Re/TiO_2$ showed almost no deactivation; however, under identical conditions, Pt/TiO_2 lost about 40% of its initial activity after 20 h time on stream [4].

3.2. Transient pulse experiments over $Pt–Re/TiO_2$ catalytic system

In order to investigate the reaction pathways and elementary steps of the WGS reaction over $Pt–Re/TiO_2$ catalyst, transient kinetic pulse studies were carried out. Fig. 2 gives the details of the pulse experiments and the response from the GC (PPQ column)–MS system, for CO and H_2O pulses over $Pt–Re/TiO_2$ catalyst at 300 °C. Fig. 3 shows the cumulative amounts of CO consumed and CO_2 formed during the pulse experiments. Values for hydrogen are based on MS response and can only be used semi-quantitatively.

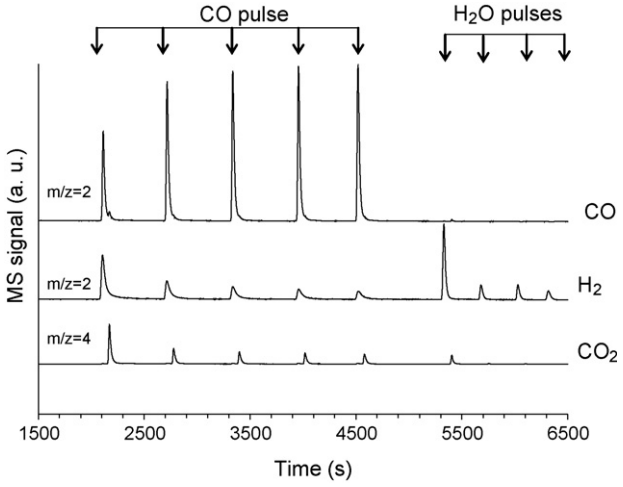

Fig. 2. MS response for pulse experiment over $Pt–Re/TiO_2$ catalyst reduced at 300 °C in H_2 (10%)/He flow. Five pulses CO are followed with four pulses H_2O. Difference in time between products detected is due to their separation with GC (porapak column).

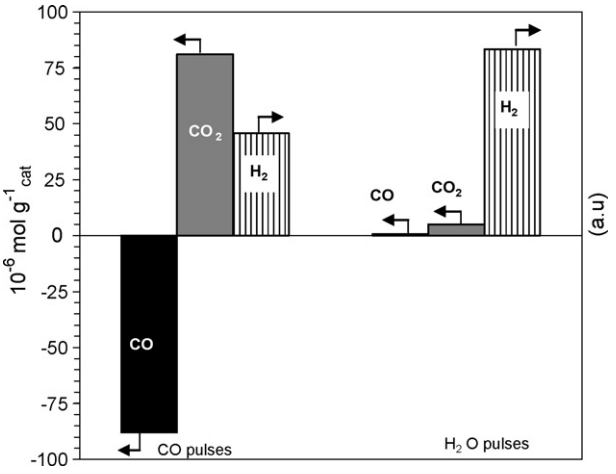

Fig. 3. Quantification of the CO and H_2O pulse results over Pt–Re/TiO_2 catalyst at 300 °C.

Contacting Pt–Re/TiO_2 with CO (Fig. 2) resulted in the simultaneous formation of CO_2 and H_2. After 5 CO pulses, only traces of CO_2 and H_2 were observed and the amount of CO detected in the outlet of the reactor (Fig. 3) was close to the amount of the pulse applied (±0.1 μmoles g^{-1}_{cat}). During the CO pulse sequence, cumulatively 88 μmoles g^{-1}_{cat} CO was consumed and 81 μmoles g^{-1}_{cat} CO_2 was formed (Fig. 3). Thus, 7 μmoles g^{-1}_{cat} CO was retained on catalyst surface.

After the CO pulse sequence, the catalyst was contacted with H_2O pulses (see Fig. 2). Contacting Pt–Re/TiO_2 with H_2O resulted in H_2 as the main product. The carbon balance of the cycle is excellent (97%, see Fig. 3) when taking into account the amounts of CO_2 formed (5 μmoles g^{-1}_{cat} whereas 7 μmoles g^{-1}_{cat} of CO was retained on the catalyst during the CO experiment). Subsequent CO–H_2O pulse cycles gave the same results.

Fig. 4 shows the *in situ* FTIR spectra recorded under conditions identical to those during CO/H_2O pulse experiments. Fig. 4a shows the IR spectra of the catalyst at 300 °C in He, *in situ,* after reduction in H_2 at this temperature. After exposure to CO at 300 °C (Fig. 4b), the band appearing at 2071 and the shoulder at 2060 cm^{-1} represent linearly adsorbed CO on Pt [22,23,27]. The shoulder at 2038 cm^{-1} corresponds to linearly adsorbed CO on Re [10,28,29] and the band at 1940 cm^{-1} indicates bridging CO on Re [10,28,29]. We have shown earlier that [4] rhenium is present in oxidized form (ReO_x) in the fresh catalyst and it cannot be reduced completely to metal below 600 °C. FTIR results indicate that rhenium is at least partially also present in metallic form after reduction at 300 °C. Bands corresponding to adsorbed carbonates and/or formates (1200–1600 cm^{-1}) were not observed. FTIR spectra recorded after H_2O pulses at 300 °C (Fig. 4c), showed only one band at 1612 cm^{-1}, which corresponds to (weakly) adsorbed H_2O on titania [30]. Fig. 5 shows the *in situ* FTIR spectra recorded under steady-state WGS reaction conditions over Pt–Re/TiO_2 catalysts at 200 and 300 °C. CO vibration region (2200–1800 cm^{-1}) looks very similar to spectra shown in Fig. 4 and therefore is not reported here. In the region typical for C–H vibrations, the bands at 2885 and 2950 cm^{-1} corresponding to the C–H stretching in formate were observed only at the lower temperature (200 °C). The fact that these bands are absent at 300 °C may indicate that formate decomposes rapidly at this temperature.

3.3. Transient pulse experiments over Pt/C and Pt–Re/C catalytic system

Supported Pt catalysts for WGS reaction are reported to be bi-functional [4,12–16] where CO activation occurs on Pt and an oxide support (e.g., TiO_2) is essential to sorb/activate water and the reaction follows Langmuir–Hinshelwood type kinetics. In order to exclude any contribution of the oxide support (TiO_2) in the activation of water during WGS cycle, we have used carbon as support and prepared two catalysts, i.e., Pt/C and Pt–Re/C. As we will show later, carbon used in this study is not an active support for WGS reaction.

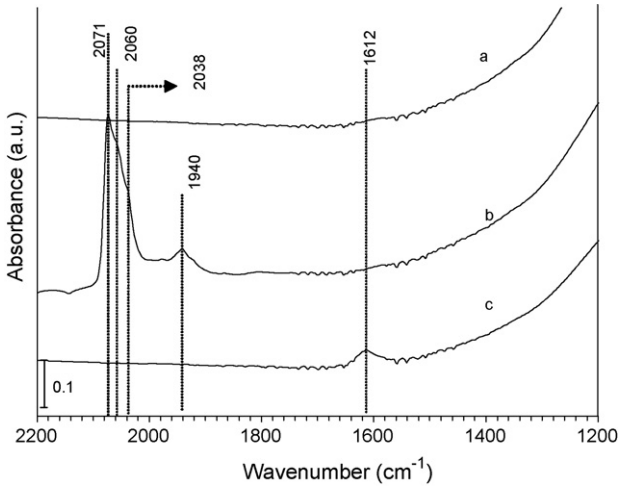

Fig. 4. *In situ* FTIR spectra at 300 °C of Pt–Re/TiO_2 catalyst; (a) reduced in 10 vol% H_2/He flow; (b) after CO pulses; (c) after H_2O pulses.

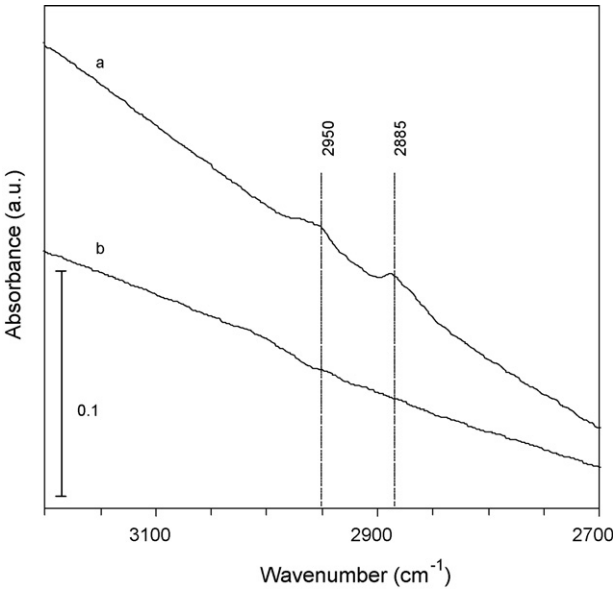

Fig. 5. *In situ* FTIR spectra of Pt–Re/TiO_2 catalyst in WGS conditions (5% CO, 10% H_2O, 85% He), total pressure of 1 atm. (a) at 200 °C and (b) at 300 °C.

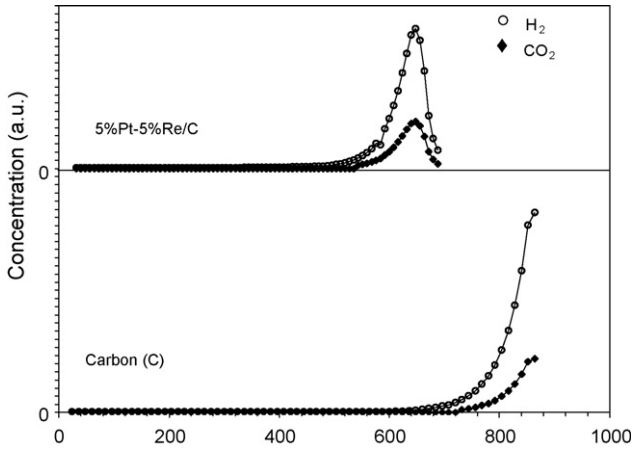

Fig. 6. GC concentration (a.u.) of H_2 and CO_2 during temperature program reaction with H_2O (5% H_2O in N_2 flow) for carbon (C) and 5% Pt–5% Re/C. Lines are just to guide the eye.

Fig. 6 shows the concentration (in a.u.) of H_2 and CO_2 formed during Temperature Programmed Reaction (oxidation) with water of carbon support and Pt–Re/C catalyst. The catalysts were heated in 5% H_2O/N_2 stream from room temperature to 650 °C for Pt–Re/C or to 850 °C in case of carbon (heating rate 3 °C min^{-1}). The outlet of the reactor was analyzed every 2.5 min with a Micro-GC. The results show that, at temperatures below 700 °C, the carbon support is stable in presence of water and no gasification took place (formation of CO, CO_2 or H_2). In the case of Pt–Re/C, H_2O reacted with carbon forming CO_2 and H_2, starting at 500 °C. These results proof that pulsing of H_2O at 300 °C over the Pt–Re/C cannot affect the carbon support. The Pt/C and Pt–Re/C catalysts were first reduced in 10% H_2/N_2 at 300 °C for 1 h prior to the pulse experiments. Pt/C did not show any activity for WGS under our conditions and accordingly, we did not observe any product (CO_2, H_2) formation during CO and H_2O pulsing. However, in the case of Pt–Re/C (Fig. 7), during the CO pulses, formation of CO_2 was observed. This is different from the case of Pt–Re/TiO_2 where we observed both CO_2 and H_2 during CO pulsing. When H_2O was introduced, both H_2 and CO_2 were observed.

Additional experiments were performed with an inert support material. Pt–Re/C catalyst was first contacted with CO at 300 °C and then heated to 400 °C in a flow of He, in order to desorb CO completely from both Pt [31,32] as well as Re (separate *in situ* IR measurements showed that CO desorption on Pt–Re/TiO_2 was complete at 390 °C). After this, pulsing H_2O resulted in formation of H_2 exclusively (Fig. 8). Furthermore, subsequently pulsing with CO resulted in CO_2 formation.

3.4. Kinetic studies for Pt–Re/TiO_2 catalytic system

Kinetic measurements were carried out according to the procedure given in the experimental section. The complete data set of concentrations are summarized in Appendix A (Table A.1). Absence of heat and mass transfer limitation were checked using the Madon–Boudart test [33]. Specifically, two catalysts with different (i) Pt, Re loadings (0.5% Pt–0.48% Re/TiO_2 and 0.3% Pt–0.3% Re/TiO_2) and (ii) comparable Pt dispersions, 50% and 58% respectively), gave identical rates for two different temperatures (TOF 15 ± 1 s^{-1} at 300 °C and 12 ± 1 s^{-1} at 280 °C for both catalysts, see Table 1). Based on these data we can exclude heat and mass transfer limitations in WGS reaction under selected conditions.

Dependence of reaction rates on the partial pressures of reactants and products, at 300 °C and 2 atm. are shown in Fig. 9. These kinetic data were fitted to the power rate law expression below, to determine the apparent reaction orders with respect to reactants and products.

$$r_{H_2} = k_f p_{CO}^a p_{H_2O}^b p_{H_2}^c p_{CO_2}^d (1-\beta)$$

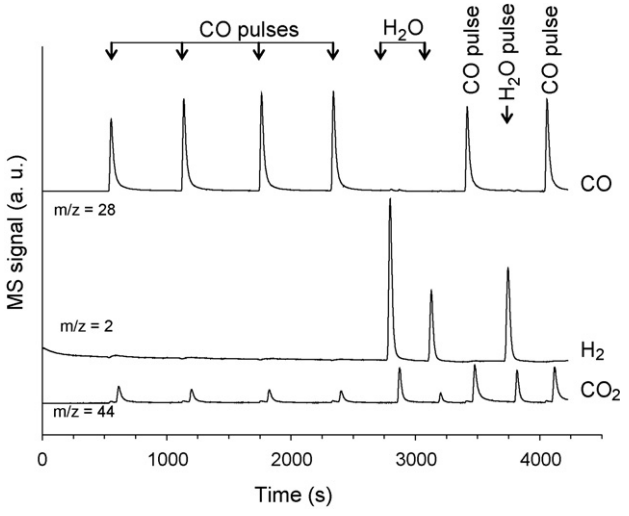

Fig. 7. MS response for pulse experiment over 5% Pt–5% Re/C catalyst reduced at 300 °C. The catalyst was reduced in H_2 (10%)/He flow at 300 °C prior to pulse experiments. Difference in time between products detected is due to their separation with GC (porapak column).

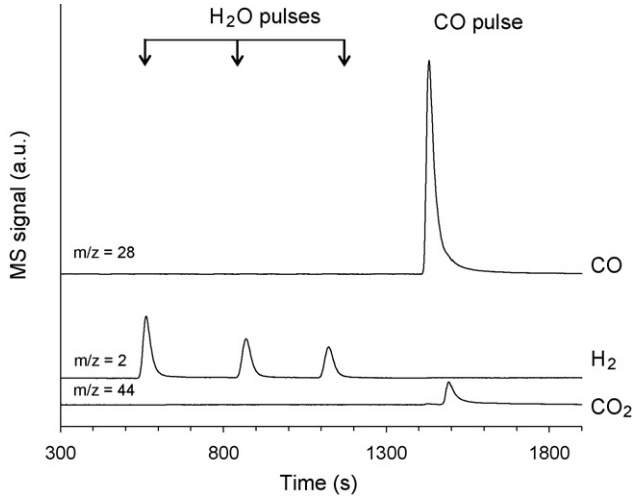

Fig. 8. MS response for pulse experiment over 5% Pt–5% Re/C catalyst. The catalyst was heated in He stream to 400 °C after CO pulses then cooled down to 300 °C prior to H_2O pulses.

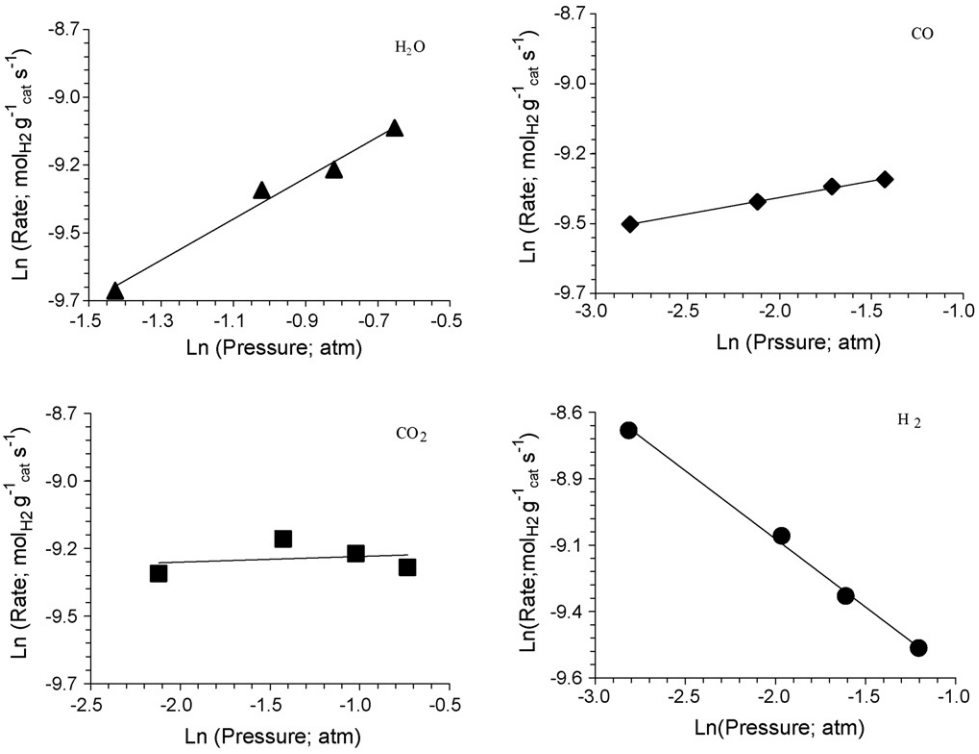

Fig. 9. Determination of power-rate law orders (WGS reaction) for Pt–Re/TiO_2 catalyst at 300 °C and 2 atm. Variation of rates with partial pressures of components (see Table A.1).

In this equation, r_{H_2} is the rate of H_2 formation, k_f is the forward rate constant, a, b, c and d are the apparent reaction orders and β is the approach to equilibrium ($\beta = p_{CO_2}\, p_{H_2}/K_{eq}\, p_{CO}\, p_{H_2O}$). The reverse reactions could be neglected (i.e., $\beta \sim 0$) as conversion was 15% maximum and thus far from equilibrium (95% conversion). The experimentally determined reaction orders are presented in Tables 2 and 3. Data in Table 2 corresponds to high CO and low CO_2 concentrations and Table 3, vice versa.

At the higher CO concentrations (Table 2), the rate was close to zero order in CO. However, at lower CO concentrations (Table 3), the reaction order of CO showed positive values (0.4). Further, the reaction was close to first order in water. Reaction rates were independent of CO_2 concentrations showing zero order kinetics. Hydrogen inhibited the reaction, showing a fractional negative order (−0.5) for the rates.

Fig. 10 shows Arrhenius plots for Pt/TiO_2 and Pt–Re/TiO_2. The apparent activation energy calculated were similar in both the cases (30 ± 1, kJ mol^{-1}).

4. Discussions

There is consensus that supported noble metal catalysts (e.g., Pt) are bifuctional in WGS, i.e., both Pt and the oxide support has roles in the catalytic sequence [4,12–16]. We have shown earlier [23], based on transient kinetic and *in situ* FTIR spectroscopic studies that on Pt/TiO_2, WGS reaction proceeds via two routes (i) a classical redox sequence in which CO reduces the oxide support and water re-oxidizes it and (ii) an

Table 2
Reaction orders of CO, H_2O, CO_2 and H_2 calculated from Fig. 9 (high CO and low CO_2 concentration)

High CO and low CO_2 concentrations			
CO[a] (±0.1)	H_2O[b] (±0.1)	CO_2[c] (±0.1)	H_2[d] (±0.1)
0.0	0.8	0.0	−0.5

[a] Concentration range: 3–12 vol%, 18% H_2O, 10% H_2, 6% CO_2 and balance N_2.
[b] Concentration range: 12–26 vol%, 12% CO, 10% H_2, 6% CO_2 and balance N_2.
[c] Concentration range: 6–24 vol%, 12% CO, 18% H_2O, 10% H_2 and balance N_2.
[d] Concentration range: 3–15 vol%, 12% CO, 18% H_2O, 6% CO_2 and balance N_2.

Table 3
Reaction order of CO, H_2O, CO_2 and H_2 (low CO and high CO_2 concentration)

High CO and low CO_2 concentrations			
CO[a] (±0.1)	H_2O[b] (±0.1)	CO_2[c] (±0.1)	H_2[d] (±0.1)
0.4	0.7	0.0	−0.4

[a] Concentration range: 1– 4 vol%, 23% H_2O, 2% H_2, 20% CO_2 and balance N_2.
[b] Concentration range: 14–23 vol%, 2% CO, 2% H_2, 20% CO_2 and balance N_2.
[c] Concentration range: 8–20 vol%, 2% CO, 23% H_2O, 2% H_2 and balance N_2.
[d] Concentration range: 2–8 vol%, 2% CO, 23% H_2O, 20% CO_2 and balance N_2.

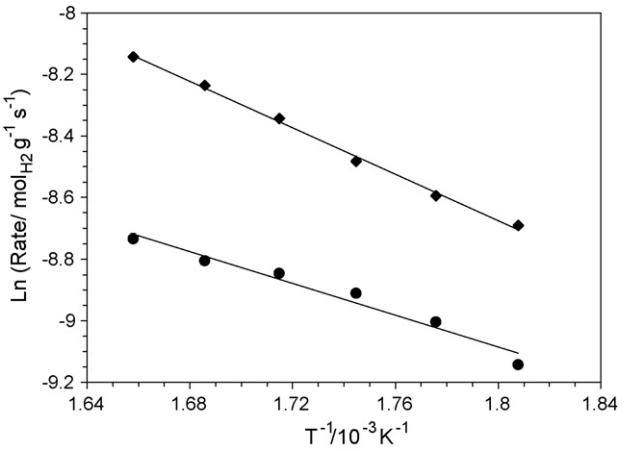

Fig. 10. Arhenius plot for the WGS reaction on 0.5% Pt–0.48% Re/TiO_2 (◆) and 0.5%Pt/TiO_2 (●). Conditions of at 1 atm. Total pressure and 3% CO, 7.5% H_2O and 89.5 vol% N_2.

associative formate route with redox regeneration. In both cases, Pt assists in the sorption/activation of CO. The reaction sequences are shown in Fig. 1.

Since addition of Re to Pt/TiO_2 enhances catalyst activity (Table 1), it is interesting to know how Re influences the reaction sequences. The results of CO and H_2O pulses (Figs. 2 and 3) over Pt–Re/TiO_2 indicate that, as in the case of Pt/TiO_2, both (i) the classical redox and (ii) associative formate route with redox regeneration are taking place. For example, formation of H_2 and CO_2 during CO pulses indicates the reaction of CO with the hydroxyl groups from the catalyst surface (Eq. (1)). Using *in situ* IR spectroscopy, we observed (Fig. 5) presence of formate type intermediates on the surface of TiO_2 during WGS reaction at 200 °C. Sato et al. [8] also observed formate intermediate on Pt–Re/TiO_2 catalyst, using *in situ* IR spectroscopy during WGS reaction, but at lower temperatures (100 °C). Moreover, Iida and Igrashi [10,24] suggested that WGS occurred via formate intermediates over Pt/TiO_2 and Pt–Re/TiO_2 catalysts. Their conclusion was based on data of *in situ* IR spectroscopy at 250 °C. Even though we did not see surface formate at our reaction conditions (300 °C), we speculate that such intermediates are still relevant, in agreement with Sato et al. [8,25] and Iida and Igrashi [10,24] The fact that contacting the catalyst with CO results in H_2 and CO_2, implies a reaction between CO and hydroxyl groups on the oxide surface, which stoichiometrically should lead to 'formate type' species. We suggest that these formates decompose rapidly (based on our observations that the catalyst is active and contains formates during WGS at 200 °C) to H_2 and CO_2 (Eq. (1)), reducing the catalyst. Formation of hydrogen during subsequent contact with water shows oxidative regeneration of TiO_2 (Eq. (2)).

$$\text{Pt}-\text{CO} + \text{OH(s)} \rightarrow \text{CO}_2\text{(g)} + 1/2\text{H}_2\text{(g)} + *\text{(s)} + \text{Pt} \quad (1)$$

$$*\text{(s)} + \text{H}_2\text{O(g)} \rightarrow \text{OH(s)} + 1/2\text{H}_2\text{(g)} \quad (2)$$

The facts that CO_2 is produced during CO pulses and hydrogen is formed in the subsequent contact with water make it impossible to exclude that the classical redox cycle contributes (Fig. 1, Eqs. (3) and (4)). Thus, the reaction sequence seems to be similar to that for Pt/TiO_2, as shown in Fig. 1. Therefore, the results of pulse studies over Pt–Re/TiO_2 indicate that the reaction mechanism is comparable with what we proposed [23] earlier for Pt/TiO_2 (Eqs. (1)–(4), and Fig. 1). Interestingly, activation energies calculated from kinetic experiments (Fig. 10) showed very similar values for both catalysts i.e., 29 kJ mol^{-1} for Pt/TiO_2 and 31 kJ mol^{-1} for Pt–Re/TiO_2.

$$\text{Pt-CO} + \text{O(s)} \rightarrow \text{CO}_2\text{(g)} + *\text{(s)} + \text{Pt} \quad (3)$$

$$*\text{(s)} + \text{H}_2\text{O(g)} \rightarrow \text{O(s)} + \text{H}_2\text{(g)} \quad (4)$$

In spite of the similarity in the mechanistic reaction sequences over the two catalysts, i.e., Pt/TiO_2 and Pt–Re/TiO_2, the latter showed higher WGS activity (Table 1). There is still debate in the literature about the reason for the higher activity of Pt–Re/TiO_2 compared to Pt/TiO_2 [8,10,24,25]. Iida and Igrashi [10,24] explain the higher activity of Pt–Re/TiO_2 catalyst due to an increase of Pt dispersion resulting from the presence of rhenium. In our case, however, Pt–Re/TiO_2 showed higher activity than Pt/TiO_2 in spite of the identical Pt dispersions ($50 \pm 3\%$) in both catalysts and identical catalyst total surface areas (Table 1). This may indicate another role for rhenium in our case. It has to be stated that (i) the Pt and Re loadings as well as (ii) Pt/Re molar ratios were different in the two studies. It is reported elsewhere [34,35] that both these factors can influence catalytic characteristics (e.g., Pt dispersion) and catalytic performance.

Alternatively, Sato et al. [8,25], based on IR results at 200 °C, attributed the enhanced activity of Pt–Re/TiO_2 to a variety of factors, viz, (i) alloy formation between Pt and Re, (ii) role of Re in stabilizing the formate and its facile transformation to H_2 and CO_2. EXAFS studies on our catalysts were inconclusive regarding Pt–Re alloy formation. Detailed studies based on (i) CO sorption and (ii) EELS to explore interaction between Re and Pt are in progress. At this moment, based on our knowledge, we cannot exclude alloy formation (Pt–Re) and its effect on catalytic activity.

Discussions below, based on our own results, consider yet another possibility for the positive influence of the presence of rhenium on catalyst activity. During CO pulses over the two catalysts, we observed higher CO_2 production in the case of Pt–Re/TiO_2 (81 and 51 μmoles g_{cat}^{-1} CO for Pt–Re/TiO_2 and Pt/TiO_2 [23], respectively). This indicates availability of extra oxygen in Pt–Re/TiO_2 catalyst.

Our XPS results [4] and that of Iida and Igrashi [10] showed that rhenium is present in oxidized form (ReO_x) in the Pt–Re/TiO_2 catalyst at ambient conditions. Temperature programmed reduction-using hydrogen [4] showed that (ReO_x) could not be reduced completely below 600 °C. Since WGS is carried out at 300 °C in the current study, at least part of the rhenium should be present in oxidized form in our working catalyst. Therefore it is reasonable to consider the possibility that oxygen from ReO_x is involved in the oxidation of CO, which can be replenished by oxygen from water, as in a re-oxidation step.

In order to establish the role, if any, of ReO_x in the Pt–Re/TiO_2 catalyst, it is necessary to exclude the role of TiO_2 (where 'redox' normally occurs during WGS cycle). Thus, CO and H_2O pulse experiments were carried out over Pt–Re/C catalyst. Since Pt/C showed no WGS shift activity (see Fig. 7a) we exclude any catalytic role for carbon in the Pt–Re/C catalyst. During CO pulses (Fig. 7b), only CO_2 was observed and as expected no hydrogen was formed. The only source available for oxygen is then ReO_x, and oxidation of CO must be by oxygen from ReO_x, (Eq. (5)). The amount of oxygen consumed to make CO_2 was less then 2% of the total oxygen available in ReO_x, assuming the stoichiometrty to be ReO_2.

$$ReO_x + Pt{-}CO \rightarrow CO_2(g) + ReO_{x-1} + Pt \quad (5)$$

$$ReO_{x-1} + H_2O(g) \rightarrow ReO_x + H_2(g) \quad (6)$$

Contacting this catalyst subsequently with H_2O resulted in the formation of H_2 and CO_2 (Fig. 7b). H_2 formation would correspond to re-oxidation of ReO_{x-1} by H_2O (Eq. (6)). This is indeed confirmed by Sato et al. [8] who reported, using *in situ* XPS characterization, the oxidation of reduced ReO_x in Pt–Re/TiO_2 catalyst by H_2O even at 100 °C.

The following arguments clarify why CO_2 was formed during H_2O pulse. It is important to recall that neither carbonate nor formate were stable on Pt–Re/TiO_2 catalyst at 300 °C (see Fig. 4). Thus, during the H_2O pulses, re-oxidation of ReO_{x-1} occurs and the CO sorbed on Pt can react with oxygen from ReO_x to form CO_2. To establish this, the catalyst was contacted with CO at 300 °C and then heated to 400 °C in He for 1 h. This allowed desorption of all CO sorbed on the catalyst [31,32]. Subsequent contact with H_2O at 300 °C, as in the earlier case, resulted in H_2 formation only (Fig. 8). The next CO pulse led to only CO_2, as expected from a classical redox cycle via ReO_x (Eqs. (5) and (6)). Repeated cycles of CO and H_2O pulses (Fig. 7b), subsequently, led to the same product distribution compared with the first cycle indicating the reduction and re-oxidation of ReO_x in the Pt–Re/C catalyst.

To summarize, we observe that the addition of Re to Pt/TiO_2 catalyst (i) does not influence the reaction sequences (ii) at least part of the rhenium is present as ReO_x and it cannot be reduced completely under at the WGS conditions used in this study and (iii) ReO_x provides an additional redox route to the reaction sequences (reduction by CO and re-oxidation by H_2O). We propose this additional redox activity to be the reason for the enhanced catalytic activity observed for Pt–Re/TiO_2. Thus, WGS on Pt–Re/TiO_2 catalyst follows the mechanistic sequence of an associative formate with redox regeneration (Eqs. (1) and (2)) and two classical redox routes, i.e., involving TiO_2 (Eqs. (3) and (4)) and ReO_x (Eqs. (5) and (6)) respectively.

Accurate description of the reaction rates with help of empirical kinetic expressions (e.g., power rate law) is essential for reactor design. Moreover, kinetic descriptions can serve as an indication of the prevalent reaction mechanism and sometimes specific mechanisms can be rejected. In this study, two data sets have been selected (Tables 2 and 3 and Figs. 9 and 10) for further discussion below.

To recall, the reaction rate was not influenced by CO_2 and CO (at high CO concentration), depended linearly on p_{H_2O} and influenced negatively (−0.5 order) by p_{H_2}. Zero order in CO implies that, at the temperature and pressure used in this study, the CO sorption is facile and CO coverage on Pt is close to complete ($\phi_{CO} \sim 1$). This is fully in agreement with previous work on Pt/CeO_2 [12,36], Pd/CeO_2 [17], Rh/CeO_2 [12], Pt/$Ce_{0.58}Zr_{0.42}O_2$ [37], and Pt/Al_2O_3 [36] all reporting zero order in CO. Therefore, CO adsorption can be ruled out as the rate determining step. In the case of low CO concentrations, reaction order in CO becomes positive (Table 3). This is also typical for zero order reactions that tend to first order at low reactant concentrations. In agreement with that, Jacobs et al. [38] also reported the increase of CO reaction order from zero to one over Pt/CeO_2 catalyst when using lower CO concentrations.

Zero order kinetics observed for CO_2 indicates that desorption of CO_2 from TiO_2, where it is formed, is fast (Pt does not adsorb CO_2 at this temperature). We have shown earlier, based on kinetic pulse transient and *in situ* IR studies [23], that carbonates are unstable on TiO_2 at the reaction temperature (300 °C) used. Wang et al. [39] also reported, using TPD measurements, the instability of carbonate on TiO_2 surface above 250 °C. Therefore desorption of CO_2 can be ruled out as rate limiting step.

The reaction order in H_2O was close to unity (0.8) independent of CO and CO_2 pressure. Water is the most difficult molecule to activate in WGS since the reaction involves splitting an extremely stable O–H bond and therefore a positive order is not surprising. Bunluesin et al. (Pt/CeO_2) [12], Phatak et al. (Pt/CeO_2 and Pt/Al_2O_3) [36], and Radhakrishnan et al. [37], (Pt–Re/$Ce_{0.58}Zr_{0.42}O_2$) also reported a first order dependence of the WGS rate on p_{H_2O}. These arguments suggest that the rate-determining step may involve water, i.e., re-oxidation of the support. The first order in p_{H_2O} might indicate that the rate is limited by re-oxidation of TiO_2 (Eqs. (2) and (4)) and/or ReO_x (Eq. (6)) by water.

WGS reaction inhibition by hydrogen, (the reaction order is −0.5) is more difficult to understand. However, the observation of a negative order in H_2 implies that application of a hydrogen-selective-membrane reactor, in order to remove hydrogen form the reaction mixture, would not only drive the conversion above the maximum conversion according thermodynamic equilibrium, but it would also enhance reaction rates. Therefore, the proposition of a hydrogen-selective-membrane reactor is a promising concept for WGS. Half order in hydrogen indicates dissociation of H_2. In principle, this impedance by hydrogen can occur at the Pt or support sites during reaction. We do not think that the rate inhibition is due to competitive adsorption between ''H'' and CO on Pt surface, in disagreement with Phatak et al. [36], because CO adsorption is known to be much more facile than ''H'' on Pt [40], e.g., CO is a strong poison for (de)hydrogenation reactions on Pt. Moreover, the zero order in CO excludes the possibility of significant competition between ''H'' and CO on Pt. The role, if any, for Pt (in case of hydrogen) will be to catalyze associative desorption (as H_2) of any hydrogen formed. Radhakrishnan et al. [37] also reported

a negative order (−0.3) in H_2 for WGS over Pt–Re/$Ce_{0.58}Zr_{0.42}O_2$ catalyst, however, no explanation was given.

Steam reforming and WGS are typical reactions involving water as a reactant. In the case of steam reforming on oxide supported nickel catalysts, water activation is reported to occur on both nickel and the support oxide (MgO–Al_2O_3) [41–43]. It has been reported that hydrogen can influence the reaction rate negatively (reaction order of (−1)), during steam reforming of hydrocarbons, by suppressing H_2O activation [41–43]. It is important to recall that bi-functional catalysis is suggested for Pt based steam reforming catalysts, in which the support plays a role in activating water [44,45]. Activation of H_2O is not thermodynamically favorable on Pt [46].

Therefore, over Pt–Re/TiO_2 catalyst, the influence of H_2 must be via the support (TiO_2) and/or via ReO_x. A separate kinetic study on Pt/TiO_2 (without Re) catalyst also showed negative order in H_2 (reaction order of −0.4). We therefore conclude that the negative influence of H_2 concentration is in suppressing activation of H_2O on TiO_2 via reactions (2) and/or (4) as explained below.

It has been suggested [47–49] that oxygen defect vacancies, in reducible oxides such as titania, can act as specific sites for H_2 activation. This results in trapped ionic hydrogen (Ti^{4+}–H^-) species [47–49]. As we showed in reaction scheme, Fig. 1, such oxygen vacancies are necessary for the activation of water, it is thus also possible that the presence of hydrogen at these vacant oxygen sites hinders activation of H_2O on these defect sites of TiO_2 via influencing the formation of OH^{-1} and/or O^{-2} (Eqs. (2) and (4)). Since this is reported to occur at lower temperatures (75 °C), we can neither confirm nor exclude this possibility.

According to the reaction mechanism proposed in the beginning of this section, however, three different reaction paths may contribute. We have used kinetic modeling of our experimental results over Pt–Re/TiO_2 to validate these reaction sequences.

Path 1:

$$Pt{-}CO + O(s) \rightarrow CO_2(g) + *(s) + Pt$$

$$*(s) + H_2O(g) \rightarrow O(s) + H_2(g)$$

Path 2:

$$Pt{-}CO + OH(s) \rightarrow CO_2(g) + 1/2H_2(g) + *(s) + Pt$$

$$*(s) + H_2O(g) \rightarrow OH(s) + 1/2H_2(g)$$

Path 3:

$$Pt{-}CO + ReO_x \rightarrow CO_{2(g)} + ReO_{x-1} + Pt$$

$$ReO_{x-1} + H_2O(g) \rightarrow H_2(g) + ReO_x$$

We have derived the rate equation for each of these paths and then simplified the rate equation by assuming rate limiting steps for each case. This allowed us to calculate the resulting apparent reaction orders and to determine which path is the dominant. Appendix B gives the details of the kinetic analyses.

Based on these analyses, in the case of the reactions occurring in Path 2, we observe convergence with experimentally observed orders. Interestingly, in this situation we also find a (−0.5) order in hydrogen and (+1) order in water. Thus, the kinetic analysis indicates that during the WGS reaction at 300 °C over Pt–Re/TiO_2 catalyst (i) Path 2 seems to be the dominant, (ii) the reaction of OH groups from TiO_2 support with CO adsorbed on Pt (Pt–CO + OH(s) → CO_2(g) + 1/2H_2(g) + *(s) + Pt) is the rate determining, and (iii) hydrogen inhibits the activation of H_2O by suppressing the formation of OH groups on TiO_2, either by shifting the equilibrium (*(s) + H_2O(g) ↔ OH(s) + 1/2H_2(g)) or by interaction of hydrogen with vacancies as discussed earlier.

5. Conclusions

In the Pt–Re/TiO_2 catalyst, rhenium is present at least partly as ReO_x, providing an additional redox route for WGS reaction in which ReO_x is reduced by CO generating CO_2 and re-oxidized by H_2O forming H_2. Thus, under the experimental conditions of this work, an associative formate route with redox regeneration (via TiO_2) as well as two classical redox routes involving both TiO_2 and ReO_x are possible reaction routes for WGS reaction.

We propose that the formate route with redox regeneration on TiO_2 is the dominant pathway and that the reaction of adsorbed CO on Pt with OH groups on TiO_2 is rate determining. Hydrogen inhibits the WGS rate by suppressing the formation of OH groups. Removing H_2 from the reaction mixture by using a hydrogen-selective-membrane reactor is promising strategy for practical applications.

Acknowledgment

The authors thank Drs. S.D. Crapanzano for the help in performing pulse experiments, Ing. L. Vrielink for XRF and BET analysis, Ing. B. Geerdink and K. Altena-Schildkamp for technical assistance. The financial support of the project by STW (project no. 790.36.030, The Netherlands) is kindly acknowledged.

Appendix A

See Table A.1.

Table A.1
Kinetic data used for reaction order calculation in the case of high CO concentration (Fig. 9)

p_{CO} (bar)	p_{H_2} (bar)	p_{H_2O} (bar)	p_{CO_2} (bar)	p_{N_2} (bar)	Rate ($\mu molH_2\ g^{-1}\ s^{-1}$)
H_2 order					
0.247	0.066	0.355	0.120	1.211	172.0
0.241	0.142	0.362	0.119	1.138	116.0
0.241	0.198	0.370	0.112	1.081	92.1
0.240	0.291	0.380	0.120	0.989	75.7
CO order					
0.241	0.198	0.370	0.112	1.081	92.1
0.173	0.192	0.360	0.122	1.153	89.8
0.115	0.192	0.363	0.121	1.211	85.1
0.057	0.191	0.366	0.120	1.267	78.5

Table A.1 (*Continued*)

p_{CO} (bar)	p_{H_2} (bar)	p_{H_2O} (bar)	p_{CO_2} (bar)	p_{N_2} (bar)	Rate ($\mu molH_2\ g^{-1}\ s^{-1}$)
CO_2 order					
0.241	0.198	0.370	0.112	1.081	92.1
0.240	0.196	0.360	0.243	0.961	104.7
0.238	0.195	0.358	0.367	0.840	99.2
0.237	0.194	0.365	0.493	0.716	94.3
H_2O order					
0.242	0.200	0.234	0.121	1.20	63.6
0.241	0.198	0.370	0.112	1.081	92.1
0.232	0.191	0.444	0.122	1.016	99.4
0.232	0.190	0.522	0.120	0.936	119.1

Appendix B. Mathematical derivation of rate equation for WGS over Pt–Re/TiO_2 catalyst

Based on the proposed reaction mechanism in this paper, three reaction sequences have been suggested.

Path 1:

$$\left.\begin{array}{l} Pt{-}CO + O(s) \rightarrow CO_2(g) + *(s) + Pt \\ *(s) + H_2O(g) \rightarrow O(s) + H_2(g) \end{array}\right\} \text{over } TiO_2$$

Path 2:

$$\left.\begin{array}{l} Pt{-}CO + OH(s) \rightarrow CO_2(g) + *(s) + Pt \\ *(s) + H_2O(g) \rightarrow OH(s) + \frac{1}{2}H_2(g) \end{array}\right\} \text{over } TiO_2$$

Path 3:

$$\left.\begin{array}{l} Pt{-}CO + ReO_x \rightarrow CO_2(g) + ReO_{x-1} + Pt \\ ReO_{x-1} + H_2O(g) \rightarrow H_2(g) + ReO_x \end{array}\right\} \text{over } ReO_x$$

From the kinetic study, we found that, in the case of high CO and low CO_2 concentrations, the reaction orders were zero order in both CO and CO_2, linear in H_2O and (−0.5) in H_2 concentrations). In the other case (low CO and high CO_2 concentrations) only the reaction order of CO is influenced (increased to 0.4) however, no significant changes occur to the reaction order of the other gases. In the comparison between the experimental data and rate derived from modeling, we will consider the reaction orders of 0, 0, 1, and −0.5 for CO, CO_2, H_2O, and H_2, respectively.

B.1. If Path 1 is the dominant:

B.1.1. CO reaction with O(s) is r.d.s.:

$$Pt{-}CO + O(s) \rightarrow CO_2(g) + *(s) + Pt$$

$$*(s) + H_2O(g) \leftrightarrow O(s) + H_2(g)$$

$$r_1 = k_1 \Phi_{CO} \theta_{Os}$$

Where k_1 is the forward rate constant, Φ_{CO} is the coverage of CO, and θ_{Os} is the coverage of oxygen on TiO_2 surface.

Rate is zero order in CO $\rightarrow \Phi_{CO} = 1 \rightarrow r_1 = k_1 \theta_{Os}$

$$k_2 \theta_* p_{H_2O} - k_{-2} \theta_{Os} p_{H_2} = 0$$

$\theta_{Os} = K_2 \theta_* p_{H_2O} / p_{H_2}$, where K_2 is the equilibrium constant of dissociative adsorptions of H_2O in the vacant sites of TiO_2 surface as O(s) and H_2(g).

$$\theta_* + \theta_{Os} = 1 \rightarrow \theta_* = 1 - \theta_{Os}$$

$$\theta_{Os} = K_2 (1 - \theta_{Os}) p_{H_2O} / p_{H_2} \rightarrow \theta_{Os}$$
$$= K_2 p_{H_2O} / (p_{H_2} + K_2 p_{H_2O})$$

$$r_1 = k_1 \frac{K_2 p_{H_2O}}{p_{H_2} + K_2 p_{H_2O}}$$

If $K_2\ p_{H_2O} \gg p_{H_2} \rightarrow r_1 =$ constant (disagree with kinetic results). If $p_{H_2} \gg K_2 p_{H_2O} \rightarrow r_1 = K_2 p_{H_2O} / p_{H_2}$ (−1 order in H_2 concentrations, disagree with kinetic results) therefore, at this both extreme situation, the reaction of CO with O_s cannot be r.d.s. It is not possible to look mathematically at intermediate situations from the current data.

*B.1.2. If the reaction of H_2O with *(s) is the r.d.s.*

$$*(s) + H_2O(g) \rightarrow O(s) + H_2(g)$$

$$Pt{-}CO + O(s) \leftrightarrow CO_2(g) + *(s) + Pt$$

$$r_1 = k_1 \theta_* p_{H_2O}$$

$k_3 \Phi_{CO}\ \theta_{Os} - k_{-3} p_{CO_2}\ \theta_*\ \Phi_* = 0 \rightarrow \theta_* \neq f(H_2)$, where K_3 is equilibrium reaction constant of the reaction of adsorbed CO on Pt with oxygen from TiO_2 surface.

This means $r_1 \neq f(H_2)$ and thus order zero in H_2 (which is in disagreement with kinetic results)

B.2. If Path 2 is the dominant

B.2.1. If CO reaction with OH(s) (r.d.s.)

$$*(s) + H_2O(g) \leftrightarrow OH(s) + 1/2H_2(g)$$

$$Pt{-}CO + OH(s) \rightarrow CO_2(g) + 1/2H_2(g) + *(s) + Pt$$

$$r_1 = k_1 \Phi_{CO} \theta_{OHs}$$

Rate is zero order in CO $\rightarrow \Phi_{CO} = 1 \rightarrow r_1 = k_1\ \theta_{OHs}$

$$k_4 \theta_* p_{H_2O} - k_{-4} \theta_{OHs} \sqrt{p_{H_2}} = 0$$

$\theta_* = \theta_{OHs} \sqrt{p_{H_2}} / K_4\ p_{H_2O}$, where K_4 is the equilibrium constant of dissociative adsorptions of H_2O to hydroxyls in the vacant

sites of TiO_2 surface

$$\theta_* + \theta_{OHs} = 1 \rightarrow \theta_{OHs} = 1 - \theta_* = 1 - \theta_{OHs}\sqrt{p_{H_2}}/K_4\, p_{H_2O}$$

$$\theta_{OHs} = \frac{K_4\left(p_{H_2O}/\sqrt{p_{H2}}\right)}{1 + K_4\left(p_{H_2O}/\sqrt{p_{H_2}}\right)}$$

$$r_1 = k_1 \frac{K_4\left(p_{H_2O}/\sqrt{p_{H_2}}\right)}{1 + K_4\left(p_{H_2O}/\sqrt{p_{H_2}}\right)}$$

If $1 \gg K_4\, p_{H_2O}/\sqrt{p_{H_2}}$, then $r_1 = k_1 K_4\left(p_{H_2O}/\sqrt{p_{H_2}}\right)$

This rate is linear in H_2O and -0.5 in H_2 concentration (in agreement with kinetic results)

B.2.2. If the H_2O reaction with oxygen vacant site is the r.d.s.

$$*(s) + H_2O(g) \rightarrow OH(s) + 1/2H_2(g)$$

$$Pt{-}CO + OH(s) \leftrightarrow CO_2(g) + 1/2H_2(g) + *(s) + Pt$$

$$r_1 = k_1 \theta_* p_{H_2O}$$

$k_5 \Phi_{CO} \theta_{OHs} - k_5 p_{CO_2} \sqrt{p_{H_2}} \theta_* = 0$, where $\Phi_{CO} = 1$

$\theta_* = K_5 \theta_{OHs}/\sqrt{p_{H_2}}\, p_{CO_2}$, where K_5 is the equilibrium reaction constant of the reaction of adsorbed CO on Pt with OH groups from TiO_2 surface.But: $\theta_* + \theta_{OHs} = 1 \rightarrow \theta_{OHs} = 1 - \theta_*$

$$\theta_* = K_5(1 - \theta_*)/\sqrt{p_{H_2}}\, p_{CO_2} \rightarrow \theta_* = K_5/(1 + K_5/\sqrt{p_{H_2}}\, p_{CO_2})$$

Then:

$$r_1 = k_1\, K_5\, p_{H_2O}/(1 + K_5/\sqrt{p_{H_2}}\, p_{CO_2})$$

If $1 \gg K_5/\sqrt{p_{H_2}}\, p_{CO_2} \rightarrow r_1 = k_1 K_5\, p_{H_2O}$ (disagree with kinetic data)

If $1 \ll K_5/\sqrt{p_{H_2}}\, p_{CO_2} \rightarrow r_1 = k_1\, p_{H_2O}\, p_{CO_2} \sqrt{p_{H_2}}$ (this rate is linearly positive in H_2O and CO_2, and also positive (0.5) in H_2, which is also in disagreement with kinetic data)

B.3. If Path 3 is the dominant:

The rate derivation of this path is comparable with the results of path 1; however, the oxygen here is involved from ReO_x instead of TiO_2. Details are thus not repeated.

This path can be ruled out as a dominant reaction path since a separate kinetic study on Pt/TiO_2 catalyst showed a -0.5 reaction order in H_2. In addition, in the case of $Re–Pt/TiO_2$ the rate of H_2 formation increases with 50% only compared to the activity of Pt/TiO_2. Note that the number of Pt and Re atoms is of the same order. Thus the redox route via ReO_x does significantly contribute, but is still not the main pathway.

B.4. Conclusion

From this modeling, path 2 seems to be the dominant path and the reaction of adsorbed CO (CO–Pt) with OH groups from TiO_2 seems to be the rate determining. The rate equation, which is derived based on this assumption, matches with experimental kinetic data.

References

[1] C.H. Bartolomew, R.J. Farrauto, Fundamentals of Industrial Catalytic Processes, John Wiley & Sons, New Jersey, 2006, p. 909.
[2] W. Ruettinger, O. Ilinich, R.J. Farrauto, J. Power. Sour. 118 (2003) 61.
[3] S. David, Catal. Rev. – Sci. Eng. 21 (1980) 275.
[4] K.G. Azzam, I.V. Babich, K. Seshan, L. Lefferts, J. Catal. 251 (2007) 163.
[5] T. Tabakova, V. Idakiev, D. Andreeva, I. Mitov, Appl. Catal. A: Gen. 222 (2000) 91.
[6] Q. Fu, H. Saltsburg, M. Flytzani-Stephanopoulos, Science 301 (2003) 935.
[7] X. Wang, R.J. Gorte, Appl. Catal. A: Gen. 247 (2003) 157.
[8] Y. Sato, K. Terada, S. Hasegawa, T. Miyao, S. Naito, Appl. Catal. A: Gen. 296 (2005) 80.
[9] G. Jacobs, L. Williams, U. Graham, D. Sparks, B. Davis, J. Phys. Chem. B 107 (2003) 10398.
[10] H. Iida, A. Igarashi, Appl. Catal. A: Gen. 303 (2006) 48.
[11] F.C. Meunier, D. Tibiletti, A. Goguet, D. Reid, R. Burch, Appl. Catal. A: Gen. 289 (2006) 104.
[12] T. Bunluesin, R.J. Gorte, G.W. Graham, Appl. Catal. B: Enviromental 15 (1998) 107.
[13] S. Yu Choung, M. Ferrandon, T. Karause, Catal. Today 99 (2005) 257.
[14] D.C. Grenoble, M.M. Estadt, D.F. Ollis, J. Catal. 67 (1981) 90.
[15] R.J. Gorte, S. Zhao, Catal. Today 104 (2005) 18.
[16] G.G. Olympiou, C.M. Kalamaras, C.D. Zeinalipour-Yazdi, A.M. Efstathiou, Catal. Today 127 (2007) 304.
[17] S. Hilaire, X. Wang, T. Luo, R.J. Gorte, J. Wagner, Appl. Catal. A: Gen. 215 (2001) 271.
[18] Y. Li, Q. Fu, M. Flytzani-Stephanopoulos, Appl. Catal. B: Enviromental 27 (2000) 179.
[19] G. Jacobs, U.M. Graham, E. Chenu, P.M. Patterson, A. Dozier, B.H. Davis, J. Catal. 229 (2005) 499.
[20] A. Goguet, S.O. Shekhtman, R. Burch, C. Hardcare, F.C. Meunier, G.S. Yablonsky, J. Catal. 237 (2006) 102.
[21] S.Y. Choung, M. Ferrandon, T. Krause, Catal. Today 99 (2005) 257.
[22] P. Panagiotopoulou, A. Christodulakis, D.I. Kondarides, S. Boghosian, J. Catal. 240 (2006) 114.
[23] K.G. Azzam, I.V. Babich, K. Seshan, L. Lefferts, J. Catal. 251 (2007) 153.
[24] H. Iida, A. Igrashi, Appl. Catal. A: Gen. 303 (2006) 192.
[25] Y. Sato, K. Terada, Y. Soma, T. Miyao, S. Naito, Catal. Comm. 7 (2006) 91.
[26] C.L. Pieck, C.R. Vera, J.M. Perera, G.N. Gimenez, L.R. Serra, L.S. Carvalho, M.C. Rangel, Catal. Today 107–108 (2005) 637.
[27] A. Holmgren, B. Andersson, D. Duprez, Appl. Catal. B 22 (1999) 215.
[28] C. Bolivar, H. Charcosset, R. Frety, M. Primet, L. Tournayan, C. Betizeau, G. Leclercq, R. Maurel, J. Catal. 45 (1976) 163.
[29] J.B. Peri, J. Catal. 52 (1978) 144.
[30] J. Steyn, G. Pattrick, M.S. Scurrell, D. Hildebrandt, M.C. Raphulu, E. van der Lingen, Catal. Today 122 (2007) 254, and references therein.
[31] P. Loof, B. Kasemo, S. Andersson, A. Frestad, J. Catal. 130 (1991) 181.
[32] B.N. Racine, M.J. Sally, B. Wade, R.K. Herz, J. Catal. 127 (1991) 307.
[33] R. Madon, M. Boudart, Ind. Eng. Chem. Fundm. 21 (1982) 438.
[34] J.L. Margitfalvi, S. Gobolos, Catalysis 17 (2004) 1.
[35] A.S. Fung, M.R. Mcdevitt, P.A. Tooley, M.J. Kelley, D.C. Koningsberger, B.C. Gates, J. Catal. 140 (1993) 190.
[36] A.A. Phatak, N. Koryabkina, S. Rai, J.L. Ratts, W. Ruettinger, R.J. Farrauto, G.E. Blau, W.N. Delgass, F.H. Ribeiro, Catal. Today 123 (2007) 224.

[37] R. Radhakrishnan, R.R. Willigan, Z. Dardas, T.H. Vanderspurt, Appl. Catal. B: Environ. 66 (2006) 23.
[38] G. Jacobs, L. Williams, U. Graham, G.A. Thomas, D.E. Sparks, B.H. Davis, Appl. Catal. A: Gen. 252 (2003) 107.
[39] J.A. Wang, A. Cuan, J. Salamones, N. Nava, S. Castillo, M. Moran-Pineda, F. Rojas, Appl. Surf. Sci. 230 (2004) 94.
[40] N.V. Pavlenko, N.I. O'chenko, Yu.I. Pyatnitskii, Theor. Exp. Chem. 33 (5) (1997) 254.
[41] R. Rostrup-Nielsen, in: J.R. Anderson, M. Boudart (Eds.), Catalysis, Science and Technology, vol. 5, Springer-Verlag, Berlin, 1984, p. 50.
[42] I.M. Bodrov, L.O. Apel'baum, M.I. Temkin, Kinet. Catal. 5 (1964) 696.
[43] I.M. Bodrov, L.O. Apel'baum, M.I. Temkin, Kinet. Catal. 9 (1968) 1065.
[44] K. Takanabe, K. Aika, K. Seshan, L. Lefferts, J. Catal. 227 (2004) 101.
[45] K. Takanabe, K. Aika, K. Inazu, T. Baba, K. Seshan, L. Lefferts, J. Catal. 243 (2006) 263.
[46] M.A. Henderson, Surf. Sci. Rep. 46 (2002) 1.
[47] W. Gopel, G. Rocker, Phys. Rev. B 28 (1983) 3427.
[48] M. Calatayud, A. Markovits, C. Minot, Surf. Sci. 524 (2003) 49.
[49] J. Leconte, A. Markovits, M.K. Skalli, C. Minot, A. Belmajdoub, Surf. Sci. 497 (2002) 194.